

# Upward-Concurrent Flame Spread over a Thin Cotton Fabric: The Effect of Ambient Pressure

Thomsen M.<sup>1</sup>, Fernandez-Pello C.<sup>1,\*</sup>, Ruff G.<sup>2</sup>, Urban D.<sup>2</sup>

<sup>1</sup>*Department of Mechanical Engineering, University of California, Berkeley, CA, 94720, USA*

<sup>2</sup>*NASA Glenn Research Center, 21000 Brookpark Rd., Cleveland, OH, 44135, USA*

\* *Corresponding author's email: [ferpello@me.berkeley.edu](mailto:ferpello@me.berkeley.edu)*

## ABSTRACT

Understanding the flammability of combustible materials at various ambient conditions is important for fire safety applications because fires may occur in environments different from standard atmosphere. In high altitude locations or in an aircraft, for example, the ambient pressure will be lower than at sea level. In the case of a spacecraft such as the International Space Station the cabin environment may be quite different, although the ambient pressure is approximately that of standard Earth, it includes microgravity, low velocity flows induced by the spacecraft ventilation. These low velocity flows (~20 cm/s) cannot be attained in normal gravity because flame induced buoyancy flows (~40 to 60 cm/s) would mask microgravity flows. Ambient pressure affects the buoyant flow induced by the flame and consequently also affects the way that flames spread. Thus, fire testing of materials may require different environments depending on the potential application of the material. The objective of this work is to provide further information of the effect of ambient pressure, and in turn buoyancy, on the upward concurrent spread of flames over a thin cotton fabric in low velocity air flows. The cotton material has been selected because it is common clothing material, and also because it will be one of the materials that will be tested in the microgravity experiments to be conducted during NASA's Spacecraft Fire Experiment (Saffire), on board of the Orbital Corporation Cygnus spacecraft.

**KEYWORDS:** Concurrent flame spread, thin fuel, ambient pressure, buoyancy.

## INTRODUCTION

The flammability of solid combustible materials is typically characterized by their ignitability, flame spread rate, heat release rate, and toxicity. Although, the most effective fire safety strategy is to prevent ignition altogether, if ignition occurs the fire must spread to present a risk. For this reason, flame spread is one of the fire processes utilized to determine the flammability of solid combustible materials [1, 2]. A flame spreads over a solid fuel surface by first preheating the virgin fuel to its pyrolysis temperature, pyrolyzing it, and igniting the resulting flammable mixture of pyrolyzate and oxygen. Thus, the flame propagates in a creeping fashion as a series of ignition steps where the flame acts both as the source of solid heating and flammable gas ignition [1–4]. Thus, the spread of flames over the surface of a solid combustible material is a complex phenomenon resulting from a number of processes occurring in both the solid phase (heat transfer, thermal decomposition, gasification) and the gas phase (transport, mixing, combustion) which are very much affected by external environmental conditions such as oxidizer flow velocity, pressure, oxygen concentration, buoyancy (gravity level) or external heating. Thus, there is an interest in studying the effect of environmental conditions on flame spread.

Concurrent, or flow assisted, flame spread occurs when the spread of the flame and the gas flow are in the same direction (upward spread in buoyant flow and downstream spread in a forced flow).

Proceedings of the Ninth International Seminar on Fire and Explosion Hazards (ISFEH9), pp. 731-740

Edited by Snegirev A., Liu N.A., Tamanini F., Bradley D., Molkov V., and Chaumeix N.

Published by Saint-Petersburg Polytechnic University Press

ISBN: 978-5-7422-6498-9 DOI: 10.18720/spbpu/2/k19-7

Because the gas flow assists the spread of the flame this mode of flame spread is generally fast and consequently hazardous. It is for this reason that some material flammability tests use this mode of flame spread to characterize the fire hazard of combustible materials. In this flame spread configuration, the solid preheating and pyrolysis rates are dominated by convection and flame radiation, and the external flow velocity will therefore influence both the flame length and the heat flux from the flame to the solid surface [3, 5–15]. Since there are marked differences in the velocity distributions in flame induced buoyant flows at different pressure [16], it is expected that there will be also notable differences in the spread of flames. The ambient pressure affects, through the density, the thickness of the boundary layer, and consequently the position of the flame respect to the solid surface (Fig. 1). As the pressure is reduced the boundary layer thickens, the flame moves away from the surface, and the heat transferred from the flame to the solid surface is reduced. Consequently, the rate of flame spread is reduced, both because the reduced heat flux on the surface and a reduction in the flame length [7]. Thus, the effect on the flame characteristics and the spread rate, of reducing the ambient pressure is similar to that of reducing the flow velocity. This is relevant because in a high-altitude location or in an aircraft, for example, the ambient pressure will be lower than at sea level. In the case of a spacecraft such as the International Space Station the cabin environment may be quite different, although the ambient pressure is approximately that of standard Earth, it includes microgravity, low velocity flows induced by the spacecraft ventilation.

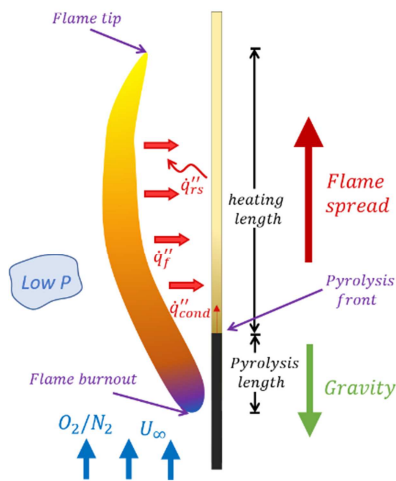


**Fig. 1.** Upward/Concurrent flame spread diagram.

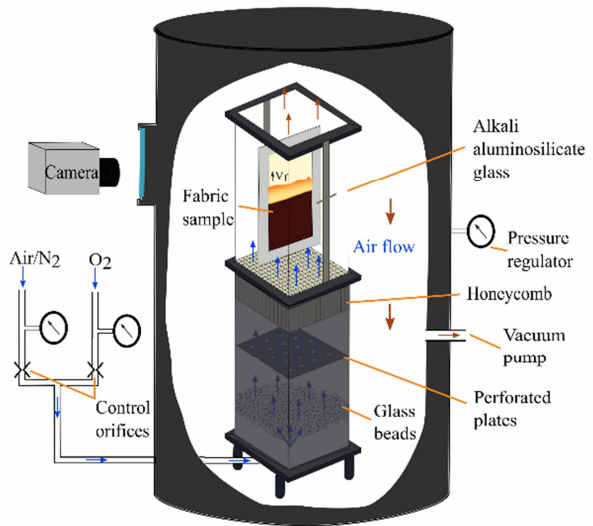


**Fig. 2.** Schematic of experimental apparatus.

Several studies have been conducted on the spread of flames over solid fuels under reduced pressure to observe the effect of buoyancy on flame spread in reduced gravity [17–21], flame spread in a high-altitude location [22–25], and limiting condition for flame spread [26, 27]. However, there is still a need to systematically study the effect of pressure, and consequently buoyancy, on the spread of flame over different solid combustible materials. The objective of this work is to determine the effect of ambient pressure on the upward concurrent spread of flames over a thin cotton fabric in low velocity air flows. The material has been selected because it is common clothing material, and also it will be one of the materials that will be tested in the microgravity experiments to be conducted during NASA's Spacecraft Fire Experiment (Saffire), on board of the Orbital Corporation Cygnus spacecraft [28]. The ambient pressures have been selected to cover a wide range of environments and buoyantly induced gas flow velocities.

## EXPERIMENTAL SETUP

The normal gravity experiments were conducted in an apparatus previously developed to study the flammability of solid combustible materials under varied ambient conditions [27]. The apparatus is basically the same as that used in the studies of Ref. [21], although modified to accept the cotton samples. A brief description of the apparatus is given here for completeness. The apparatus consists of a laboratory scale combustion tunnel that has a 125 mm by 125 mm cross section and is 600 mm in total length. The first 350 mm section of the duct serves as a flow straightener, the other 250 mm segment of the duct is used as the test section. The tunnel is inserted in a pressure chamber as shown in Fig. 2. The side walls of the test section (normal to the plane of the samples) are made of clear polycarbonate. The walls parallel to the sample are 0.56 mm thick alkali-aluminosilicate glass. The sample is placed vertically at the midplane of the test section with both sides exposed to the flow. The fabric sample is made out of pure cotton and has an overall area density of  $21.8 \text{ mg/cm}^2$ . The sample material and configuration was selected to match one of the materials that will be used in future Saffire microgravity experiments [28]. The cotton samples were 150 mm long by 50 mm wide. The sample was held in between two identical stainless-steel frames of 200 mm by 125 mm and 0.4 mm thick. Each frame had an identical rectangular opening the size of the sample to serve as the test area. Sample ignition is induced with a 29-gage Kanthal wire braided along the upstream edge of the fabric as shown in Fig. 3. The igniter is energized using a controlled current power supply (BK Precision 1785) set to deliver 40 W, the time required to assure ignition changed depending on the ambient pressure tested but was between 3 to 10 seconds.

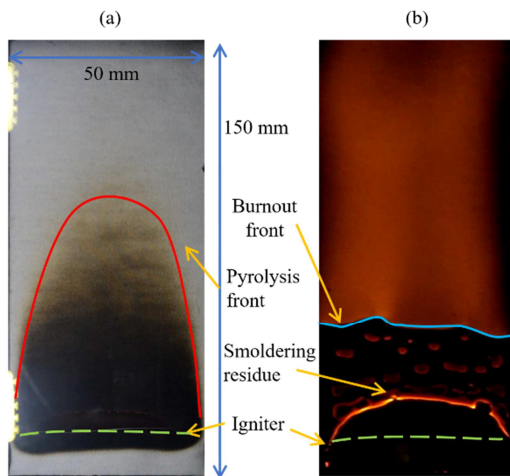


**Fig. 3.** Front view showing two representative frames of a video of the flame spread over the cotton surface (a) pyrolysis front, and (b) flame burnout front.

The tests were conducted in air under pressures of 100, 80, 70, 50, and  $30 \pm 2$  kPa. Compressed house air was supplied through critical nozzles (O’Keefe Controls) while constantly evacuating to maintain constant the pressure inside the chamber. The chamber pressure was controlled by a high-capacity vacuum generator (Vaccon JS-300) and a mechanical vacuum regulator. The chamber pressure was monitored constantly with an electronic pressure transducer (Omega Engineering, Inc. PX303-015A5V). The forced flow velocity was fixed to 20 cm/s in all the tests. The direction of the flow was upward so that the spread of the flame was in the concurrent configuration. The forced flow velocity was selected to match that to be tested in the microgravity Saffire experiments. Once the sample was in position, the chamber was sealed to adjust the system to the desired conditions. Two 9000 lumen LED were installed with an operating electronic circuit to act as a strobe light to

visualize and measure during the same experiment flame spread rates and the flame appearance. The ignition and subsequent flame spread were video recorded with a resolution of 1280 by 720 at 59 frames per second using a Nikon D3200 camera to track the pyrolysis front. A second camera (Sony RX10-III) was used to record videos of visible flame length with a resolution of 1280 by 720 at 59 frames per second. For each test condition, at least five experiments were conducted to address the experimental uncertainty.

## RESULTS

Concurrent flame spread over cotton was investigated under different ambient pressures. The primary data collected were the evolution of the pyrolysis front and burnout front positions over time (Fig. 1). The flame tip was not recorded because it was difficult to determine accurately its location with time. Representative frames with the flame spreading over the cotton sample are shown in Fig. 3. Figure 3a presents a frame with the strobe light on and shows the pyrolysis front. Here, the position of the pyrolysis front was defined as the point where the fabric is first visibly blackened as it propagates over the material. Figure 3b presents a frame with the light off and shows the flame burnout front as well some cotton residue smoldering after the passing of the flame. Here, the burnout front position was defined as the upstream edge of the flame, which coincides with where the flame begins receding. During each test, after ignition is achieved, the flame spreads uniformly along the surface of the sample. The pyrolysis front had an inverted "U" shape in all tests, while the flame burnout front had a flatter, more unstable shape. Usually, after ignition of the sample, as the flame spreads over the fabric it consumes most of the cotton, leaving behind some smoldering cotton residue (bottom of Fig. 3b) that eventually burns out most of the fabric. As ambient pressure was reduced, ignition of the sample was more difficult, and, in occasions, part of the cotton fabric would be left unburnt.

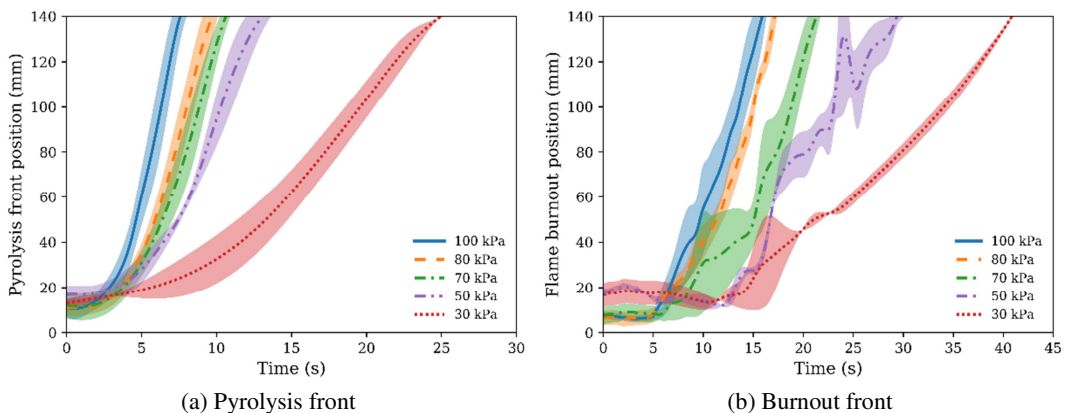


**Fig. 4.** Time evolution of the (a) pyrolysis front position and (b) flame burnout position for different ambient pressures.

Some characteristic results of the time evolution of the pyrolysis front and burnout front are presented in Fig. 4 for ambient pressures ranging from 100 to 30 kPa. Figure 4a shows the progress of the pyrolysis front as a function of time. It is seen that as ambient pressure is reduced the spread of the flame is slower. During most of the tests, the flame is still accelerating as it spreads over the solid. The work of Markstein and De Ris [5] indicates that this is due to the sample not being long enough to reach steady state. Similar results to those presented in this work were presented by the authors using a different material, a composite cotton/fiber glass fabric (Sibal) [21]. When comparing the characteristics of the flame spread of Thomsen et al. [21] with a longer Sibal sample

reported by Olson et al. [20] (samples of 0.15 m vs. 1 m) it showed that despite the similarities in the pyrolysis front and burnout front profiles, the sample size was not long enough for the flame spread to reach steady state. However, as pressure was reduced, the pyrolysis front and flame burnout front begin to stabilize faster. From Fig. 4 is seen that the average total burn time for an initial pressure of 100 kPa was 16 s, significantly smaller when compared to the average 41 s obtained at an ambient pressure of 30 kPa.

The evolution of the pyrolysis front as a function of time is commonly used to determine flame spread rate. The data of Fig. 4 is then used to obtain average flame spread rate values as a function of ambient pressure, as shown in Fig. 5. Because of the acceleratory characteristics of the upward flame spread, an averaged spread rate over the last 50 mm of the sample is presented in the figure so that transient effects are minimized. It is seen that the flame spread rate decreases from 30.7 to 10.0 mm/s as the ambient pressure is decreased from 100 to 30 kPa.

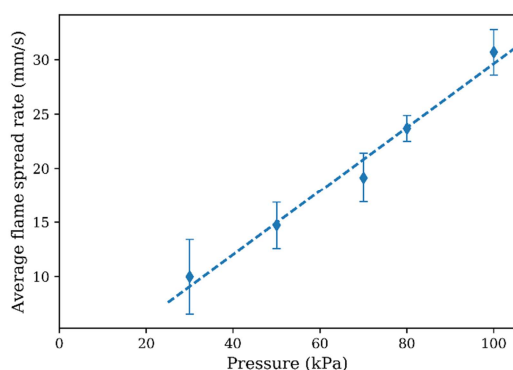


**Fig. 5.** Average flame spread rate as a function of ambient pressure obtained from the pyrolysis front.

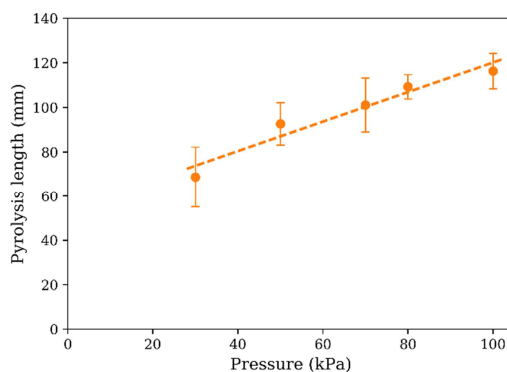


**Fig. 6.** Pyrolysis length as a function of ambient pressure.

Another important parameter for concurrent flame spread is the pyrolysis length because it determines the flame length and consequently the heat that can be transferred from the flame to the solid. In this work, this length is obtained by subtracting the burnout front position from the pyrolysis front position, and the results are presented in Fig. 6. Because of the accelerative characteristic of the spread process, the pyrolysis length is obtained toward the end of the test when it approaches steady state. From Fig. 6 it is seen that the pyrolysis length decreases from 116.4 to 68.7 mm with decreasing ambient pressure from 100 to 30 kPa. This indicates that ambient pressure affects more the rate of spread of the pyrolysis front than the mass burning, since it determines the rate of spread of the burnout front.

The visible flame characteristics also change with decreasing ambient pressure, although changes are less noticeable when compared with the flames generated by the burning of other materials [21]. Figure 7 shows still photographs of the material burning under different pressure environments. As pressure is reduced the flame becomes less turbulent and its intensity is reduced. As pressure is reduced, visible flame height is also affected, becoming shorter at lower pressures.

## DATA CORRELATION

The above data can be used to verify the predictive capabilities of flame spread models on the effect of pressure, or buoyancy, on the concurrent spread of flames over a thin combustible fuel. This was done in Ref. [21] by correlating the data of the dependence on pressure of the concurrent flame spread rate over a composite cotton/fiberglass fabric (Sibal) using the simplified analysis of Ref.

[3]. Here a similar approach is followed to correlate the cotton data presented in Figs. 5 and 6. Since the development of the data correlation was presented in [21], only a summary is presented here.



**Fig. 7.** Visible flame as a function of ambient pressure.

The flame spread analysis is based on the main controlling mechanisms for concurrent flame spread over a thin solid and treats the spread process as a sequence of ignitions where the flame acts as a source of heat to the solid and the pilot for ignition [1–4]. The analysis provides an analytical equation for concurrent flame spread over a thin solid as [3, 21]:

$$V_f = l_h \left[ \frac{\rho_s c_s s (T_p - T_o)}{h (T_f - T_p) + \dot{q}_{fr}'' - \dot{q}_{rs}''} - \frac{Cx}{U_m} \varphi(t_{chem}) \right]^{-1} \quad (1)$$

Where  $l_h$  is the heated length (Fig. 1),  $h(T_f - T_p)$  represents the convective heat flux at the solid surface,  $\dot{q}_{fr}''$  is the flame radiant flux,  $\dot{q}_{rs}''$  the re-radiation from the solid.  $U_m$  is the mixed flow velocity and  $\varphi(t_{chem})$  is a function of the chemical time,  $t_{chem}$ .  $\rho_s$  and  $c_s$  are the solid density and specific heat and  $s$  is the solid thickness.  $T_f$  is the flame temperature, and  $T_p$  and  $T_o$  are the pyrolysis and initial temperatures of the solid. The first term inside the parenthesis in Eq. (1) describes the heat transfer mechanisms of the flame spread process and the second term represents the gas phase chemical kinetics. Although reducing pressure will eventually affect the chemical kinetic process [21], it will be assumed here that for the present experimental conditions the spread rate is controlled by heat transport effects only. It is also assumed that the radiant flux from the flame to the solid is approximately balanced by the surface re-radiation, and that there is not an external heat flux. The heated length is approximately related to the pyrolysis length that  $l_h \sim C_1 l_p^c$ , where  $C_1$  is a constant and the exponent  $c$  is one or less than one [29]. The flame temperature is directly proportional to the ambient oxygen concentration but is not strongly dependent on ambient pressure until the pressure is relatively low and the chemical time starts to become larger than the physical time. Because the oxygen concentration is that of air for all the experiments, the flame temperature is assumed constant in the range of pressures of the present experiments. This is a simplification in the analysis that should be reasonable for not too low ambient pressures. Under these conditions the flame spread rate becomes:

$$V_f \approx l_p \left[ \frac{h(T_f - T_p)}{\rho_s c_s s (T_p - T_o)} \right] \quad (2)$$

From Eq. (2) it is seen that the flame spread rate is proportional to the convective heat transfer coefficient at the solid surface, which in turn is directly related to the boundary layer thickness through  $h = k/\delta$ , where  $k$  is the gas thermal conductivity and  $\delta$  the boundary layer thickness. For a mixed flow, forced and free, as that of the present experiments, the average convective heat transfer coefficient can be expressed in terms of the Reynolds Number ( $Re$ ) and the Grashof number ( $Gr$ ) as [30]:

$$h = C \frac{k}{l_p} Gr^{1/4} \left( \frac{Re^4}{Gr^2} + 1 \right)^{1/8} Pr^{1/3} \quad (3)$$

Where  $C$  is a generic constant related to the type of flow and the pyrolysis length,  $l_p$ , has been selected as the characteristic length of the problem. Then,  $Re = \rho U_f l_p / \mu$ ,  $Gr = g \beta \Delta T l_p^3 \rho^2 / \mu^2$ , and  $Pr$  is the Prandtl number.  $U_f$  represents the forced flow velocity component of the mixed flow,  $\mu$  is the dynamic viscosity,  $\rho$  is gas phase density,  $\beta$  is the coefficient of thermal expansion and  $g$  is gravity level.

Since the flame spread rate is determined primarily by the heat flux on the fuel surface, the normal gravity and the microgravity data could be related by defining a mixed flow gas velocity such that when applied to a purely forced flow, like in the microgravity experiments, would produce a boundary layer of the same thickness as that encountered by the flame in the mixed flow condition in normal gravity. Since the boundary layer thickness is directly related to the heat transfer coefficient through  $h = k/\delta$ , then the heat transfer coefficients would be the same and thus the flame spread rate would also be the same. This mixed flow velocity can be obtained by equating the heat transfer coefficient for a mixed flow as in Eq. (3) and that of a pure forced flow obtained from Eq. (3) with  $g=0$ , and solving for the flow velocity in the forced flow boundary layer. Then, the following mixed convection velocity,  $U_m$ , is obtained in terms of pressure, forced flow velocity in the mixed flow, and gravity.

$$U_m = U_f \left( \frac{P}{P_0} \right) \left[ \frac{g^2 l_p^2}{U_f^4} + 1 \right]^{1/4} \quad (4)$$

where  $P_0$  is a reference ambient pressure (standard Earth ambient pressure) and  $U_f$  is the forced flow velocity at this reference pressure  $P_0$ . From Eq. (4) it is seen that for zero gravity or large flow velocity the mixed flow velocity is that of a pure forced flow at a given test pressure,  $U_m = \frac{P}{P_0} U_f$ . For elevated gravity and/or zero forced velocity, the mixed flow velocity becomes that of natural convection at a given test pressure,  $U_m = \frac{P}{P_0} (g l_p)^{1/2}$ . With the mixed flow velocity as given in Eq. (4), the convective heat transfer coefficient for the forced flow, based on the mixed flow velocity, would be

$$h = C \frac{k}{l_p} \left( \frac{U_m P l_p}{\mu} \right)^{1/2} Pr^{1/3} \quad (5)$$

And the flame spread would be given by

$$V_f \approx l_h \frac{\left( \frac{Ck}{l_p} \left( \frac{U_m P l_p}{\mu} \right)^{1/2} Pr^{1/3} \right) (T_f - T_p)}{\rho_s c_s S (T_p - T_o)} \approx \frac{C_1 k \left( \frac{U_m P l_p}{\mu} \right)^{1/2} Pr^{1/3} (T_f - T_p)}{\rho_s c_s S (T_p - T_o)} \quad (6)$$

The flame spread data of Fig. 5 can be correlated in terms of the mixed convective flow velocity,  $U_m$ , given by Eq. (4), as shown in Fig. 8. It is seen that Eq. (4) correlates well the variation of the flame spread rate with pressure. As ambient pressure is decreased, the calculated mixed flow velocity is also reduced, and this is reflected in slower flame spread rates. A similar analysis can also be done with the experimental data presented in Fig. 6 for the pyrolysis length as shown in Fig. 9.

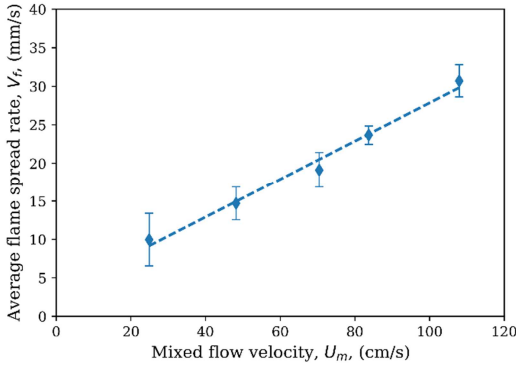


**Fig. 8.** Average flame spread rate as a function the mixed flow velocity.

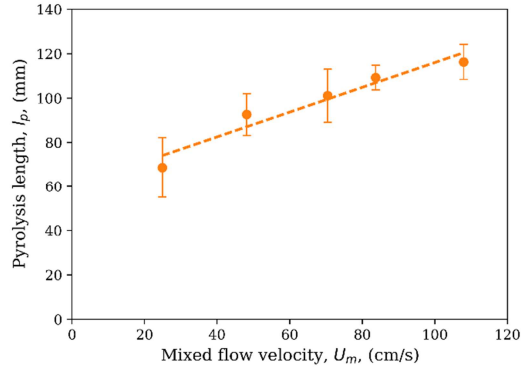


**Fig. 9.** Pyrolysis length as a function the mixed flow velocity.

**Table 1. Cotton properties [31]**

Property	Value	Units
Solid density, $\rho_s$	417	kg/m <sup>3</sup>
Solid specific heat, $c_s$	1.380	kJ/(kg·K)
Material thickness, $s$	$5.08 \times 10^{-4}$	m
Pyrolysis temperature, $T_p$	629	K
Flame temperature, $T_f$	2500	K

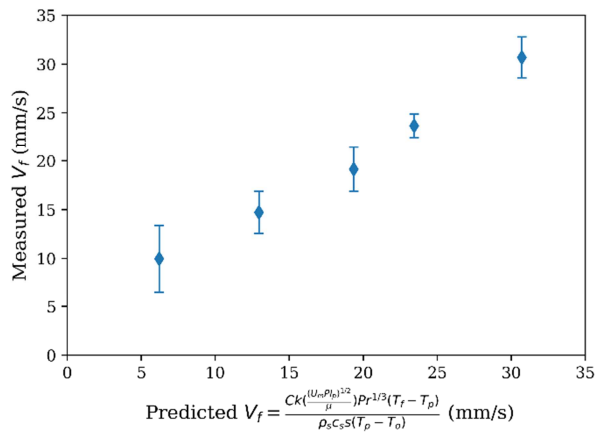


**Fig. 10.** Measured average flame spread rate as a function the predicted flame spread rate obtained from Eq. (6).



Additionally, the experimental results of Fig. 5 can be used to compare with the predictions obtained from Eq. (6). This is shown in Fig. 10 where the measured average flame spread rate is presented as a function of the predicted flame spread rate of Eq. (6). For the calculations, the cotton properties were taken as those of thin cellulose paper [31] and are presented in Table 1, the flame temperature is taken as the paper adiabatic flame temperature [31]. The value of the constant  $C_f$  was set to match the experimental flame spread rate measured at normal ambient pressure (100 kPa). From Fig. 10 it is seen that Eq. (6) predicts fairly well the experimental flame spread rates obtained in lower pressure environments. However, the flame spread results are slightly underpredicted and the differences seem to get bigger at lower pressures.

## CONCLUSIONS

The concurrent flame spread rate over a thin cotton fabric has been studied under reduced ambient pressure to determine the effect of buoyancy on the flame spread process. It has been found that as pressure is reduced, the flame spread rate over the cotton fabric is also reduced, as observed with other thin fuels [21, 32]. Flame intensity is also weakened resulting in dimmer flames. The measured flame spread rate is correlated well in terms of a simple flame spread formula and a mixed convection heat transfer coefficient. The correlation of the flame spread rate data in terms of a mixed flow velocity parameter that includes gravity and pressure suggests that reduced pressure can be used to simulate the effect of buoyancy on the concurrent spread of flames.

## ACKNOWLEDGMENTS

This research is supported by NASA Grant NNX12AN67A. The authors would like to thank Saul Pacheco, Grace Mendoza, Runbiao Wei, Ryan So, Mina Fanaian, and Madison Hales for their contributions conducting the experiments.

## REFERENCES

- [1] F.A. Williams, Mechanisms of fire spread, Symp. Combust. 16 (1976) 1281–1294.
- [2] J. Quintiere, A simplified theory for generalizing results from a radiant panel rate of flame spread apparatus, Fire Mater. 5 (1981) 52–60.
- [3] C. Fernandez-Pello, The solid phase, in: G. Cox (Ed.), Combustion Fundamentals of Fire, Academic Press Limited, 1994, pp. 31–100.
- [4] M.A. Delichatsios, Creeping flame spread: energy balance and application to practical materials, Symp. Combust. 26 (1996) 1495–1503.
- [5] G.H. Markstein, J. De Ris, Upward fire spread over textiles, Proc. Combust. Inst. 14 (1973) 1085–1097.
- [6] M. Sibulkin, J. Kim, The dependence of flame propagation on surface heat transfer II. upward burning, Combust. Sci. Technol. 17 (1977) 39–49.
- [7] A.C. Fernandez-Pello, A theoretical model for the upward laminar spread of flames over vertical fuel surfaces, Combust. Flame 31 (1978) 135–148.
- [8] A.C. Fernandez-Pello, Flame spread in a forward forced flow, Combust. Flame 36 (1979) 63–78.
- [9] L. Chu, C.H. Chen, J.S. T'ien, Upward propagation over paper samples, in: Proc. ASME Pap. 81-WA/HT-42, 1981.
- [10] H.T. Loh, C. Fernandez-Pello, A study of the controlling mechanisms of flow assisted flame spread, Proc. Combust. Inst. 20 (1984) 1575–1582.
- [11] K. Saito, J.G. Quintiere, F.A. Williams, Upward turbulent flame spread, Fire Safety Science – Proceedings of the First International Symposium, pp. 75–86 (1986).
- [12] H.T. Loh, A.C. Fernandez-Pello, Flow Assisted Flame Spread over Thermally Thin Fuels, Fire Saf. Sci. 1 (1986) 65–74.

- [13] L.K. Honda, P.D. Ronney, Mechanisms of concurrent-flow flame spread over solid fuel beds, *Proc. Combust. Inst.* 28 (2000) 2793–2801.
- [14] M.J. Gollner, X. Huang, J. Cobian, A.S. Rangwala, F.A. Williams, Experimental study of upward flame spread of an inclined fuel surface, *Proc. Combust. Inst.* 34 (2013) 2531–2538.
- [15] M.J. Gollner, C.H. Miller, W. Tang, A.V. Singh, The effect of flow and geometry on concurrent flame spread, *Fire Saf. J.* 91 (2017) 68–78.
- [16] C.K. Law, S.H. Chung, N. Srinivasan, Gas-phase quasi-steadiness and fuel vapor accumulation effects in droplet burning, *Combust. Flame* 38 (1980) 173–198.
- [17] P. V. Ferkul, J.S. T'ien, A model of low-speed concurrent flow flame spread over a thin fuel, *Combust. Sci. Technol.* 99 (1994) 345–370.
- [18] J. Kleinhenz, I.I. Feier, S.Y. Hsu, J.S. T'ien, P. V. Ferkul, K.R. Sacksteder, Pressure modeling of upward flame spread and burning rates over solids in partial gravity, *Combust. Flame* 154 (2008) 637–643.
- [19] Y. Nakamura, N. Yoshimura, H. Ito, K. Azumaya, O. Fujita, Flame spread over electric wire in sub-atmospheric pressure, *Proc. Combust. Inst.* 32 (2009) 2559–2566.
- [20] S.L. Olson, S.A. Gokoglu, D.L. Urban, G.A. Ruff, P. V. Ferkul, Upward flame spread in large enclosures: Flame growth and pressure rise, *Proc. Combust. Inst.* 35 (2015) 2623–2630.
- [21] M. Thomsen, C. Fernandez-pello, D.L. Urban, G.A. Ruff, S.L. Olson, On simulating concurrent flame spread in reduced gravity by reducing ambient pressure, *Proc. Combust. Inst.* 37 (2019) 3793–3800.
- [22] Y. Zhang, X. Huang, Q. Wang, J. Ji, J. Sun, Y. Yin, Experimental study on the characteristics of horizontal flame spread over XPS surface on plateau, *J. Hazard. Mater.* 189 (2011) 34–39.
- [23] Y. Zhang, J. Ji, J. Li, J. Sun, Q. Wang, X. Huang, Effects of altitude and sample width on the characteristics of horizontal flame spread over wood sheets, *Fire Saf. J.* 51 (2012) 120–125.
- [24] J. Gong, L. Yang, X. Zhou, Z. Deng, G. Lei, W. Wang, Effects of low atmospheric pressure on combustion characteristics of polyethylene and polymethyl methacrylate, *J. Fire Sci.* 30 (2012) 224–239.
- [25] J. Gong, X. Zhou, Z. Deng, L. Yang, Influences of low atmospheric pressure on downward flame spread over thick PMMA slabs at different altitudes, *Int. J. Heat Mass Transf.* 61 (2013) 191–200.
- [26] A.F. Osorio, C. Fernandez-Pello, D.L. Urban, G.A. Ruff, Limiting conditions for flame spread in fire resistant fabrics, *Proc. Combust. Inst.* 34 (2013) 2691–2697.
- [27] M. Thomsen, D.C. Murphy, C. Fernandez-pello, D.L. Urban, G.A. Ruff, Flame spread limits (LOC) of fire resistant fabrics, *Fire Saf. J.* 91 (2017) 259–265.
- [28] G. Jomaas, J.L. Torero, C. Eigenbrod, J. Niehaus, S.L. Olson, P.V. Ferkul, G. Legros, A.C. Fernandez-Pello, A.J. Cowlard, S. Rouvreau, N. Smirnov, O. Fujita, J.S. T'ien, G.A. Ruff, D.L. Urban, Fire safety in space – beyond flammability testing of small samples, *Acta Astronaut.* 109 (2015) 208–216.
- [29] K. Tu, J.G. Quintiere, Wall Flame Heights with External Radiation, *Fire Technol.* 27 (1991) 195–203.
- [30] C.-P. Mao, A.C. Fernandez-Pello, P.J. Pagni, Mixed convective burning of a fuel surface with arbitrary inclination, *J. Heat Transf.* 106 (1984) 304–309.
- [31] Y.T.T. Liao, J.S. T'ien, A numerical simulation of transient ignition and ignition limit of a composite solid by a localized radiant source, *Combust. Theory Model.* 17 (2013) 1096–1124.
- [32] M. Thomsen, X. Huang, C. Fernandez-Pello, D.L. Urban, G.A. Ruff, Concurrent flame spread over externally heated Nomex under mixed convection flow, *Proc. Combust. Inst.* 37 (2019) 3801–3808.